Synthesis of Black Magnetic Electrophoretic Particles for Magnetic-Electric Dual-Driven Electronic Paper

Xianwei Meng,*,[†] Li Qiang,[†,‡] Xiaofang Su,[†,‡] Jun Ren,[†] and Fangqiong Tang*,[†]

[†]Laboratory of Controllable Preparation and Application of Nanomaterials, Technical Institute of Physics and Chemistry, Chinese Academy of Sciences, Beijing 100190, People's Republic of China

[‡]University of the Chinese Academy of Sciences, Beijing 100049, People's Republic of China

ABSTRACT: The application of electronic paper (e-paper) is now propelling the development of the multifunctional e-paper products. There is an extraordinary diversity of basic and applied research in pursuit of the novel e-paper. Here, we report the first achievement of a magnetic-electric dual-driven e-paper, using black magnetic electrophoretic particles (BMEPs). BMEPs are synthesized via a facile, green, low-cost, one-step method. By adjusting the reaction conditions, the density, surface, and magnetic properties of the BMEPs are optimized for e-paper display. Finally, the e-paper display is successfully assembled using dispersion of the BMEPs in a

TIPC logo electrophoretic display switching by electric field.

mixed dielectric solvent with white particles as contrast. Thanks to the magnetic properties and a positively charged surface, the BMEPs can be driven by both electric and magnetic fields. The prototype display is fabricated whose switch is achieved by the application of either a bias voltage of 10 V or a magnetic bias. The as-prepared magnetic-electric dual-driven device could have many promising applications in the field of anticounterfeiting labels for secure identification documents.

KEYWORDS: E-paper, dual driving, electrophoretic particles, ultrasonic spray pyrolysis

1. INTRODUCTION

Since Ota and co-workers introduced a new reflective type of display based on electrophoresis,[1] electronic paper (e-paper) has been substantial researched and has reached a remarkable state of maturity.[2−4] One of the main factors driving the growth of research on e-paper is its advantages.[5,6] The reflective technology gives e-paper superior optical contrast in direct sunlight, an ink-like appearance, and reduced eyestrain.[7−10] Most of all, the near-zero-power operation is the primary concern.[11] In an e-paper display, the electrophoretic particles are required to migrate reversibly between the electrodes driven by an electric field.[12,13] The migration results in either the "white" or "black" state of the display. Thus, the display properties of e-paper are mainly determined by the composition, size, light scattering properties, and density of the electrophoretic particles.[14] Many studies have focused on synthesizing new electrophoretic particles to improve the display properties. Cho[15] described the coating of TiO_2 with polystyrene via miniemulsion polymerization. The resulting TiO_2/PS core/shell nanoparticles had lower density, which could match the dielectric medium and had better dispersion stability. Kim[16] and Yu[17] introduced a two-stage dispersion polymerization technique to encapsulate TiO_2 particles with negative charge surface functionality. The density of TiO_2 decreased from 4.0 g/cm^3 to 1.5−2.5 g/cm^3, matching well with the suspending medium. Feng[18] developed a way of fabricating yellow CdS/wax nanocomposite spheres in an aqueous solution via an emulsion method, in which the CdS

nanoparticles were adsorbed on the surface of a wax core by an electrostatic self-assembly. To enhance the optical and mechanical properties and the charge load of the composite spheres, a thin shell of SiO_2 was then coated onto the yellow CdS/wax spheres. The coating layers could effectively prevent the aggregation of CdS crystals, so the SiO_2/CdS/wax spheres had a low density, strong durability, and better optical properties and display performance. Our group has reported the design and preparation of white, black, and RGB tricolor ink particles for EPDs. All the electrophoretic particles possessed characteristics of narrow distribution, high surface charge density, and superior light stability.[19−21] The global e-paper market experienced significant growth in the year 2009 on account of the success of the E-Reader market. However, commercial e-paper stalled due to the wild popularity of the iPad. In order to break through the plateaus and gain further development, new technologies are required to endow e-paper with novel properties and applications. To our best knowledge, there has no report on the use of the magnetic properties of the electrophoretic particles for e-paper display. The magnetic-electric dual-driven display is a novel e-paper. The prototype device first assembled by us switches from one state to the other by driving not only a bias voltage but also a magnetic bias by a magnet. The dual driving gives this novel type of e-paper a
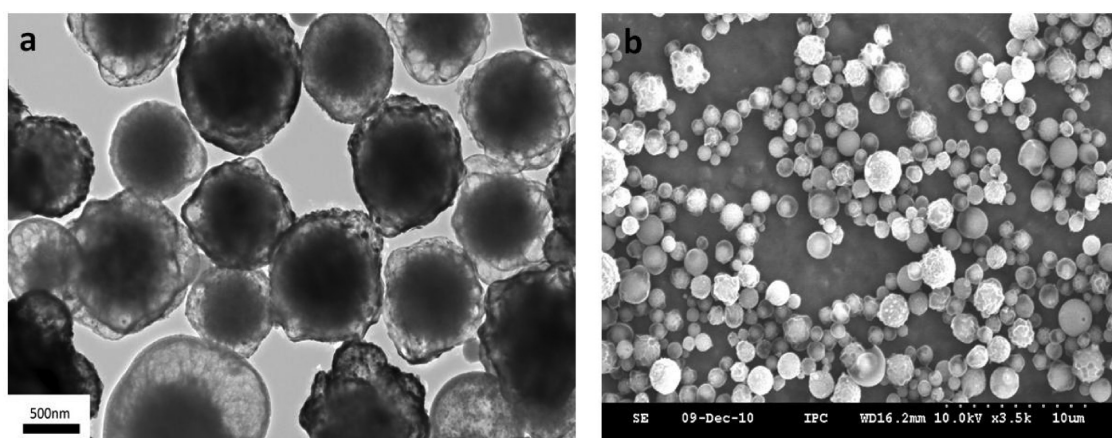
Figure 1. TEM and SEM images of the particles prepared via an ultrasonic spray pyrolysis process at different scales: (a) TEM image and (b) SEM image.

promising application to the field of anticounterfeiting labels for secure identification documents such as passports and driver's licenses. The label's customized image makes this possible with an optically variable device, an overt safety feature which come into sight to "float" above or "sink" below the facade of the label as the electric/magnetic field changes. Verification of our counterfeit label is completed easily within seconds, without having to use a complicated tool.

In this contribution, we have successfully assembled magnetic-electric dual-driven e-paper based on black magnetic electrophoretic particles (BMEPs) and TiO_2 particles. The idea for this study is based on the fact that the BMEPs can respond not only to an electric field but also a magnetic field. We demonstrated that the magnetic ingredient is Fe_3O_4 and the BMEPs have good magnetic response. The BMEPs are synthesized via an ultrasonic spray pyrolysis method. The BMEPs are carbon and magnetite core−shell structure nanocomposites whose density is ~1.5 g/cm^3. The essential requirement for the stability of the electronic ink is the compatibility between the electrophoretic particle and the disperse medium. Thanks to the superdispersant BK164, the BMEPs are well-dispersed in a dielectric solvent (a mixture of tetrachloromethane and Halocarbon 1.8 oil) with TiO_2 particles as white particles to form an electrophoretic suspension. Finally, the electrophoretic suspension is successfully incorporated in an electrophoretic display cell and a dual-driven e-paper display is achieved. The results obtained suggest that the BMEPs are applicable in both electric-field- and magnetic-field-driven displays.

2. EXPERIMENTAL SECTION

Materials. All the reagents used in this work were products of analytical purity, and they are used without further purification. Glucose, ferrous chloride, and tetrachloromethane were obtained from Beijing Chemical Works. Halocarbon with a density of 1.8 kg/L was supplied by Halocarbon Product Corporation. Titanium dioxide was purchased from Dupont Company as the sample named R-706. The BK series dispersants used in the work were from BYK Chemie; T151A, T154A, and T161A were from Tianhe Chemicals; and CH-1A, CH-2C, CH-3, and CH-5 were supplied by Shanghai San Zheng Co.

Procedures and Characterization. The black electronic particles are synthesized via an ultrasonic spray pyrolysis

method.[22] A specific synthesis method is as follows. First, the precursor solution containing a certain amount of glucose and ferric chloride with a molar ratio of 1:1 was carefully transferred to the ultrasonic equipment. Second, the precursor was nebulized into microdroplets by a 1.7-MHz ultrasonic generator (Yuyue 402AI, Shanghai Yuyue Co., Ltd.). Third, with the help of an inert gas of N_2, the mist was carried into the furnace (Model SK2-4-12A, Tianjin Zhonghuan Company) at a designated rate through a quartz tube. Under the high temperature of the furnace, the reaction took place and black electronic particles were obtained during the solvent evaporation. The product then was collected and washed by deionized water.

Transmission electron microscopy (TEM) (Model JEM-2100, JEOL) and scanning electron microscopy (SEM) (Models 4300 and 4800, Hitachi) were used to characterize the surface morphology. Powder X-ray diffraction (XRD) measurements were performed on a D8 Focus X-ray diffractometer with a scanning rate of 0.02°/s; Fourier transform infrared spectrometry (FTIR) (Varian, Model 3100 Excalibur) was employed to examine the composition of the hybrid microspheres. X-ray photoelectron spectroscopy (XPS) (ESCALAB Model 250Xi) is also applied to determine the surface functional group of the BMEPs. The thermogravimetric analysis (TGA) of the samples was monitored using Diamond TG/DTA equipment from Perkin−Elmer Company under a stream of air. The particles were heated from 30 °C to 800 °C at the rate of 10 °C/min. The magnetic hysteresis loops of the samples were recorded on a Physics Property Measurement System (Model PPMS-9, Quantum Design Co.). The particle size was measured by a Malvern Zetasizer 3000HS device. The viscosity was measured using an Ubbelohde viscometer. The change in dielectric constant was determined by dielectric constant measurement, using a device from Beijing Zhongxi Corp.

The electrophoretic suspension was prepared using a dispersion of black and white particles in a dielectric solvent (a mixture of tetrachloromethane and Halocarbon 1.8 oil), with the presence of dispersants T161A and BK164. Tetrachloromethane and Halocarbon 1.8 oil were first mixed at the ratio of 2:1 to obtain the electrophoretic solvent. Four weight percent (4 wt %) BMEPs, 10 wt % TiO_2 particles, BK164, and T161A were added. By sonicating, the electrophoretic particles were
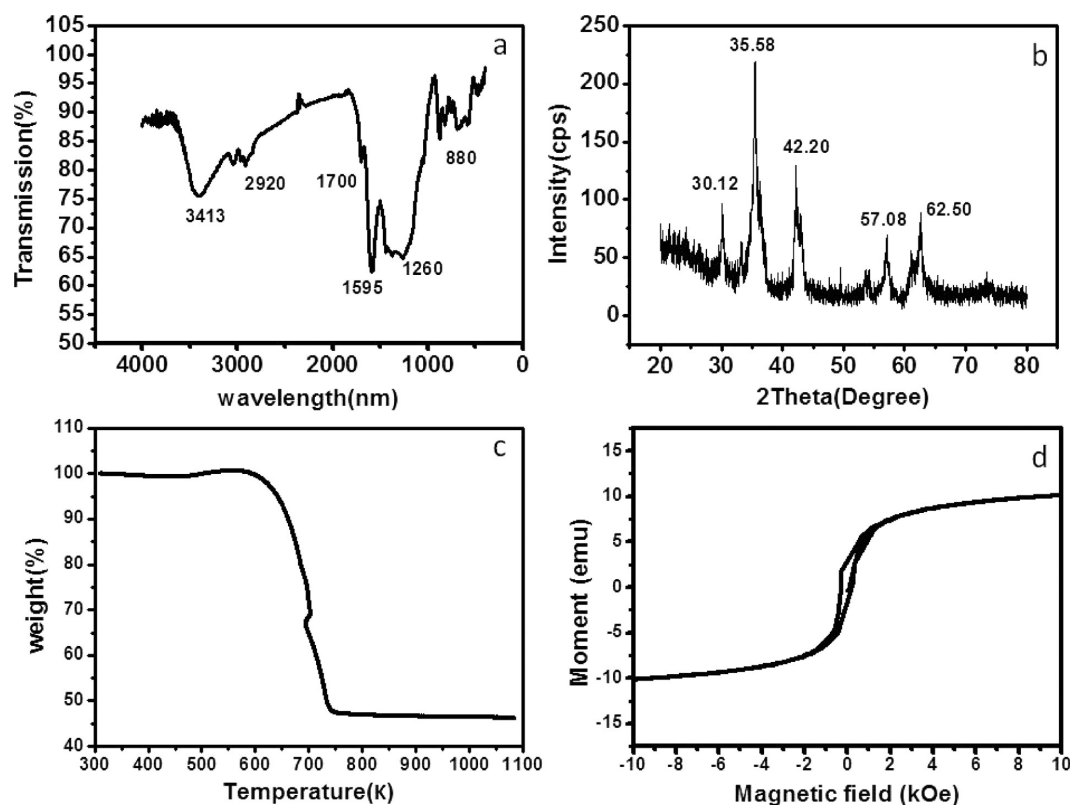
Figure 2. Characterization of the black magnetic electrophoretic particles (BMEPs): (a) FTIR, (b) XRD pattern, (c) TGA curve, and (d) the $M-H$ hysteresis loop.

well-dispersed and a uniform electrophoretic suspension was prepared.

The performance of our BMEPs was analyzed in two different display cells: an electrophoretic display cell and a magnetic-electric dual-driven display cell. The electrophoretic display cell was a device composed of a printed circuit board (PCB), as the baseboard at one side, with an electrode logo of TIPC on it. The other side is a plane ITO-covered glass slice (the scheme is shown latter in Figure 7c). The cell was filled with the electrophoretic suspension. The magnetic-electric dual-driven display cell was composed of two parallel ITO-covered glass slices; both of them are planar, and one was covered by a black Traditional Peking Opera Mask film. The cell was filled with the as-prepared electrophoretic suspension (see Figure 9a, presented later in this work). The magnetic-electric dual-driven display cell can achieve the black and white switch. The black and white contrast was measured by a UV/vis/NIR spectrophotometer (JASCO, Model V-570) under reflection mode in 5 min with shifting eight times. The response time was characterized by an Admesy Colorimeter Application.

3. RESULTS AND DISCUSSION

The BMEPs are synthesized via ultrasonic spray pyrolysis process. This is a facile, green, low-cost, one-step method. The experimental device can work sequentially and continuously to produce large-scale BMEPs. The morphology of the BMEPs is investigated by SEM and TEM. From Figure 1a and 1b, the morphology of the BMEPs can be observed, which exhibits a core−shell structure by the obvious contrast between the dark core and the fluffy shell. Figure 1b shows that the BMEPs are composed of a large quantity of microspheres. Through

calculating the particles sizes in the TEM image of Figure 1a, we obtained the mean particle size is 884 nm, with a standard deviation of 13.1%. By changing the concentration ratio of the glucose and ferric chloride in the precursor, the density of the BMEPs can be tuned to be ~1.5 g/cm³, which matches with that of the electrophoretic suspension dielectric solvent.

FTIR and XPS analyses are used to characterize the surface property of the BMEPs. The material's surface functional groups determine its polydispersity in various solvents. As shown in Figure 2a, the peaks at 3400−3500 cm⁻¹ and 2800−3000 cm⁻¹ are characteristic peaks for O−H stretching and C−H stretching, respectively. The peak at 1700 cm⁻¹ is the characteristic C=O stretching mode infrared peak. The broad peaks at 1000−1400 cm⁻¹ are characteristic peaks for C−O stretching. The FTIR spectra of the particles show the =C−H bending vibration near 880 cm⁻¹. The peaks at ~580 cm⁻¹ are characteristic peaks for magnetite.[23,24] The XPS spectrum also indicates the BMEPs have a C=O double bond in the surface shell. The C 1s photoelectron spectra contain an sp² hybridization component at lower binding energies and an sp³ hybridization component at higher binding energies. The sp³ component can be convoluted by Gaussian functions, and the sp² component is fitted to a Doniach−Sunjic function.[25] This result demonstrates that the BMEPs have a carbon double bond, which is consistent with the FTIR result. Thanks to the presence of =C−H, C=O, and C−H groups in BMEPs, they exhibit good affinity in a dielectric solvent.[24]

Figure 2b shows the XRD pattern of the BMEPs. All the diffraction peaks can be indexed to either face-centered cubic (fcc) Fe_3O_4 (JCPDS File Card No. 48-1487) or cubic γ-Fe_2O_3 (JCPDS File Card No. 39-1346). No obvious impurity phase, such as nonmagnetic α-Fe_2O_3, can be detected in Figure 2b.
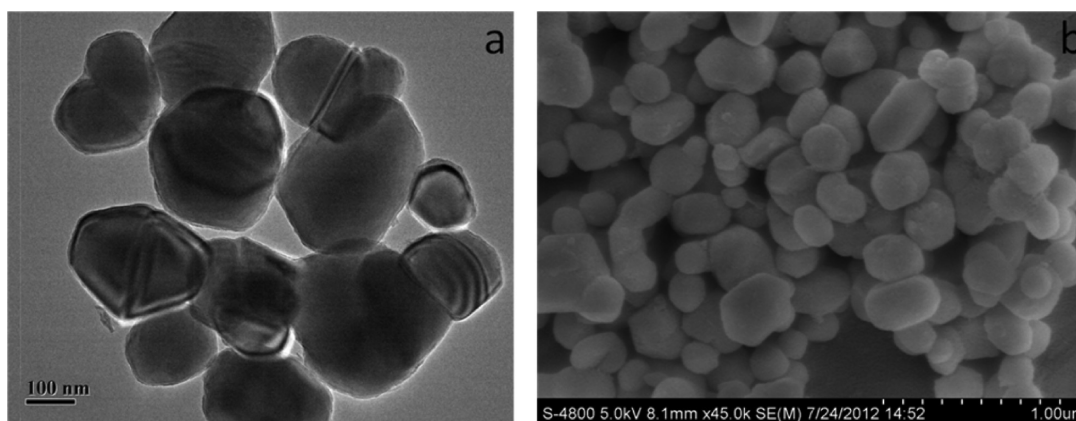

Figure 3. (a) TEM and (b) SEM images of TiO_2 particles at different scales.
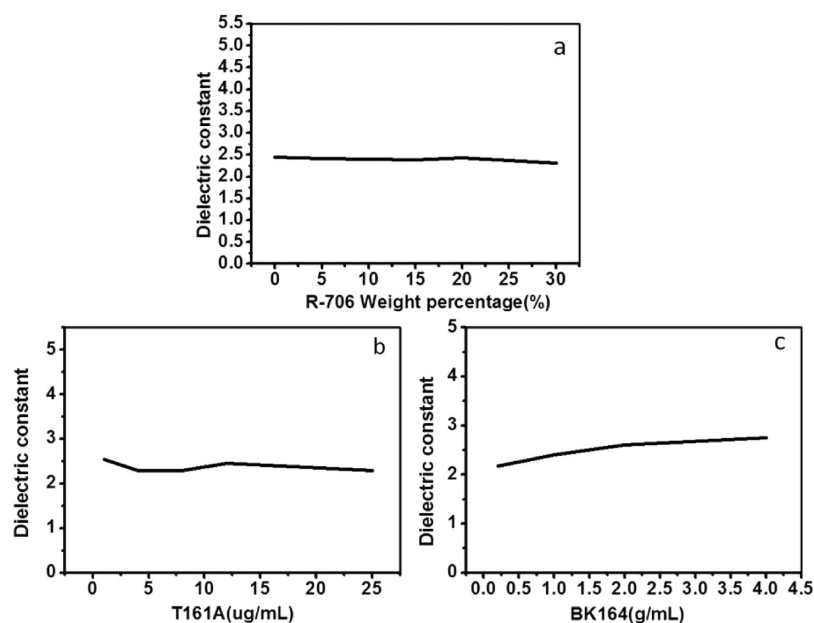

Figure 4. Dielectric constant change of electrophoretic suspension at different amounts of (a) electrophoretic particles, (b) superdispersant T161A, and (c) superdispersant BK164.

The TGA curve of the BMEPs is shown in Figure 2c. There are three main temperature regions of weight change. The weight loss below 220 °C can be attributed to the evaporation of physically absorbed water and residual solvent in the samples. In the range of 220−320 °C, the slight increase can result from the conversion of ferriferous oxide to ferric oxide. The weight loss in the temperature region of 320−460 °C can correspond to the loss of CO_2, because of the oxidation of the carbon in BMEPs. The percentage of carbon and ferriferous oxide is 50% and 49%, respectively, which can be calculated from the thermogravimetric curve. The BMEP density is 1.5 g/cm³, which is similar to the dielectric solvent. The magnetic properties of the BMEPs are characterized using a Physics Property Measurement System. As shown in Figure 2d, based on the $M-H$ hysteresis loop, the saturation magnetic field intensity of the BMEPs exhibits up to 13.8 emu g⁻¹, and the remnant magnetization (M_r) is equal to 2.2 emu g⁻¹, which is relatively low, and the coercive field (H_c) is equal to 193 Oe. From the narrow hysteresis loop, we can see that the coercivity H_c of the black particles is small, so they are very easy to be magnetized and demagnetized, which is consistent with the

characteristics of soft magnetic materials. The reason that the saturation magnetization (M_s) is lower than that of bulk Fe_3O_4 (92 emu g⁻¹) can be attributed to the small size of Fe_3O_4 nanoparticles and the presence of a nonmagnetic component (carbon, 49 wt %). This saturation magnetic field of the particle is proper to have a good magnetic response, and to avoid the magnetic attractive conjunction.

The black electrophoretic particles have optimal density, surface property, and magnetic response for being used as a magnetic-electric dual-driven e-paper display. To achieve good black and white contrast to the BMEPs, TiO_2 particles (R-706 from Dupont) are used as white electrophoretic pigment particles, which are always the best choice, because of many advantages. TiO_2 has significant optical reflection and is stable in many chemical environments. The sample TiO_2 particles are mainly pure TiO_2 with surface modification. With the presence of the surface modification, TiO_2 is more stable and easier to disperse. The electron microscope images of TiO_2 particles are shown in Figure 3. Through the images, we can see that the TiO_2 are uniform. In order to give the electrophoretic suspension a good property, mixed solvents are always
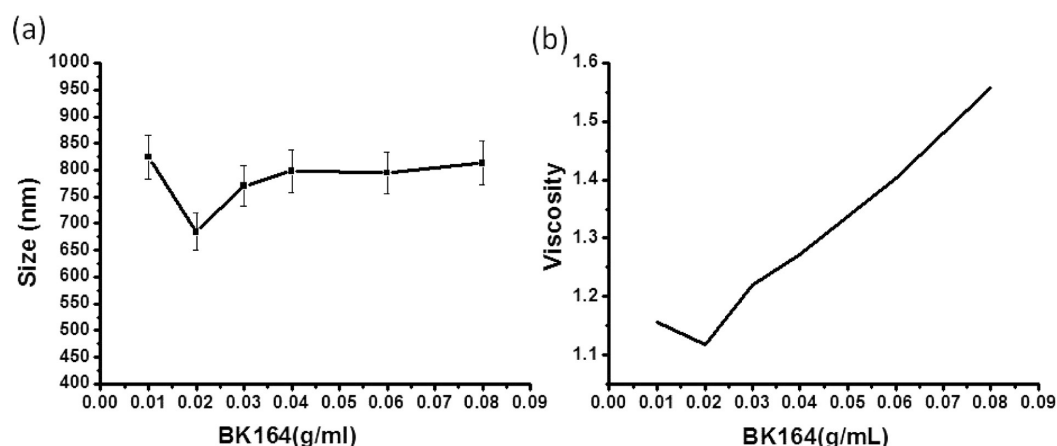
Figure 5. (a) Size of the BMEPs and (b) suspension viscosity changes at the different concentration of BK164.
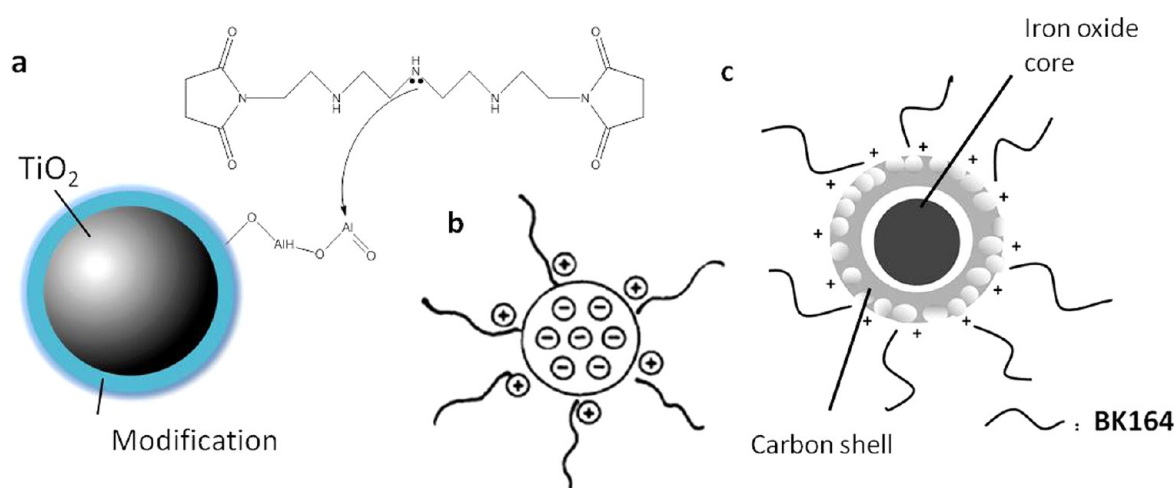

Figure 6. (a) Anchoring group and adsorbance mechanism of the superdispersant T161A on a TiO$_2$ surface in a nonaqueous dispersion system. (b) The scheme of the TiO$_2$ particles with T161A in the suspension. (c) The scheme of the BMEPs particles with BK164 in the suspension.

used.[26] The black and white electrophoretic particles are dispersed in the mixture of tetrachloromethane and Halocarbon 1.8 oil. The density and affinity of the mixed solvent are appropriate as an electrophoretic suspension solvent. When choosing the e-paper solvents, many factors must be considered, such as the density, lack of color, and low cost. Among them, the dielectric constant is very important, for the reason that the electrophoretic suspension is required to be nonpolar in order to avoid the circuit board electrolysis. Tetrachloromethane proves to be a proper solvent with low dielectric constant. Its dielectric constant has no obvious changes when the electrophoretic suspension ingredients are added. Figure 4 shows the dielectric constant change of electrophoretic suspension with an increasing amount of particles and superdispersants.

To further improve the stability of the electrophoretic particles in the dielectric mixture, a dispersant is required. There are many types of superdispersant supplied by the chemical company that can obviously improve the particle dispersibility. In this report, BK190, BK164, BK154, BK184, BK111, T151A, T154A, T161A, CH-1A, CH-2C, CH-3, and CH-5 have each been used. Among these dispersants, BK164 is the most effective dispersant for BMEPs. The BK164 is a type of polymer superdispersant that contains an anchoring functional group and a soluble polymeric long chain. Because

of the structural features, BK 164 is bound to the surface site, forming durable adsorption layers on the BMEPs. The polymer chain can spread out into the solvent, so that they generate a steric barrier that prevents particles from aggregating. Thanks to the long polymer chains of the adsorption layers, the BMEPs suspension shows good dispersibility.

Figure 5 shows the effect of BK164 dispersant concentration on the BMEPs size and the viscosity in the electrophoretic suspension with 4.0 wt % BMEPs. Figure 5a is a dynamic light scattering (DLS) measurement to determine the Z-average mean size of the BMEPs at different BK164 concentrations. It can be seen that increasing the amount of dispersant makes the mean size of the particles first decrease gradually to a minimum value, observed for 2.0 wt % dispersant, followed by an increase for further additions. The viscosity decreases with increasing BK164 content at a concentration below 2.0 wt %, beyond which, however, a significant increase in viscosity is observed to occur with increasing BK164 content. Two dispersive forces are occurring in the electrophoretic suspensions: steric hindrance and an electrostatic repulsive force.[27−29] It is of great importance that the dispersant BK164 prevents the particles from the interactions induced by the short-range factors, which is readily done through a steric hindrance mechanism. The electrostatic repulsive forces reduce the attractive forces in the secondary minimum. The BMEPs suspension with 2 wt %
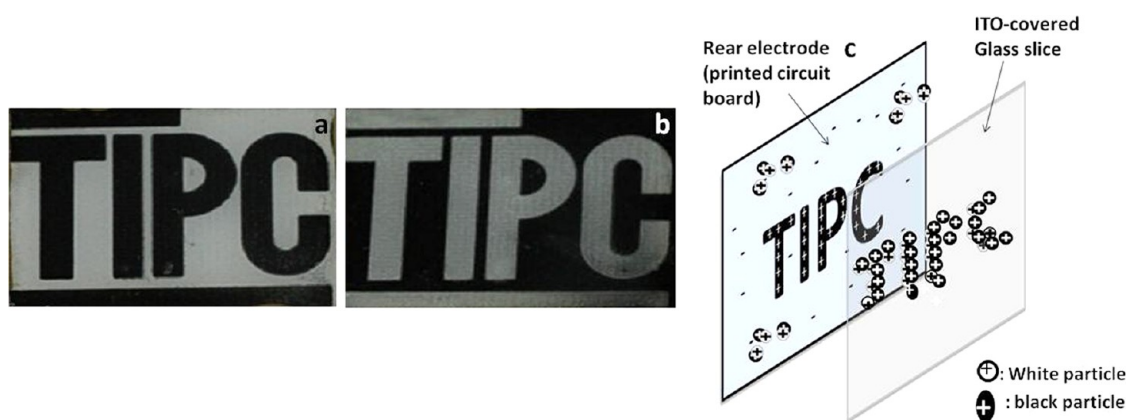
Figure 7. (a, b) Photographs of TIPC logo displayed by the electrophoretic display cell by switching the bias voltage. (c) The scheme of this electronic display cell.
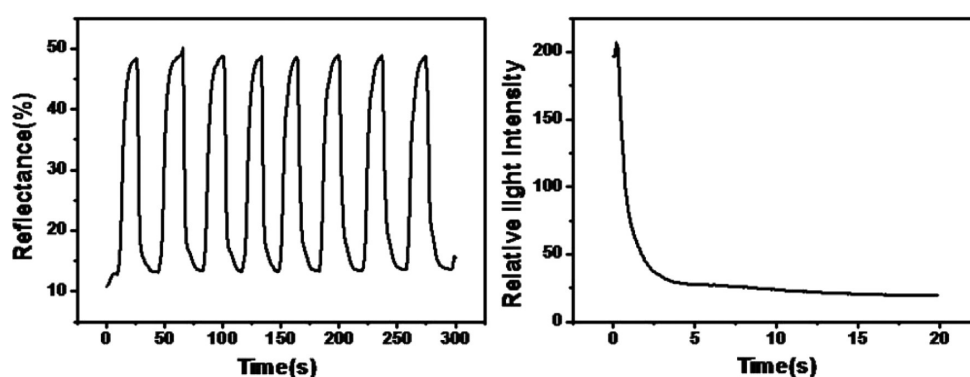
**Figure 8.** (a) Reflectance curve and (b) response time of the display cell.

BK164 shows good dispersibility, because of the saturation adsorption of the dispersant. Thus, the minimum of BMEPs size and suspension viscosity occurs at 2 wt % BK164. When further adding BK164, bridging between polymer chains may happen, resulting in that the polymer shell cannot be effectively solvated and the aggregation of particles occurs. The particles size and suspension viscosity gradually increases as particle aggregation increases. When the dispersant concentration is <2 wt %, the adsorption does not reach the saturation, because of a lack of dispersant concentration. The amount of dispersant adsorbed on the particle surface is not enough to disperse the BMEPs and the aggregation of particles occurs.

It is found that superdispersant T161A gives TiO_2 good dispersibility in the dielectric solvent. T161A is a high-molecular-weight polyisobutylene succinimide dispersant. With the good properties of temperature stability and long-chain steric stability, T161A is used as a superdispersant in the electrophoretic suspension. R-706 is a product from Dupont Company that is pure TiO_2 with alumina and silica surface treatment. The oxygen attached to the aluminum draws the electron pair closer to it, because of the greater electronegativity. This makes the Al atom somewhat electron deficient, and sharing the lone pair of electrons offered by T161A becomes easier, as shown in Figure 6a. The alumina existence on the surface of TiO_2 also increases the iep value, which make it easier for TiO_2 to take charge.[30] Therefore, the fast adsorption of T161A on the surface of TiO_2 not only increases the steric hindrance but also gives TiO_2 electric charges, which results in a good dispersion effect of the electrophoretic particles in the hydrocarbon medium. A scheme of the adsorption between T161A and TiO_2 is shown as Figure 6b. The optimal T161A amount is determined by the infrared measurement.

T161A has a characteristic infrared absorbance peak at 1705 cm^{-1} (C=O stretching peak), while the mixed solvent and the TiO_2 particles have no obvious absorbance at 1705 cm^{-1}. Therefore, we can measure the supernatant infrared absorbance intensity at 1705 cm^{-1} to determine the T161A amount adsorbed on the TiO_2 particles. After a certain concentration of T161A is fully absorbed with the TiO_2 particles, we centrifuge the suspension and collect the supernatant liquid. We use the external standard method to determine the standard curve of the infrared absorbance at different concentration of T161A; K is the infrared absorbance ratio ($K = A_{1705}/A_{standard}$, where A_{1705} is the absorbance peak at 1705 cm^{-1}, and $A_{standard}$ is the absorbance at 1379 cm^{-1} as the standard peak. The absorbance intensity shows a linear relationship with the T161A concentration. So the amount of T161A adsorbed on the particle surfaces can be measured by the infrared absorbance intensity at 1705 cm^{-1}. T161A absorbance reaches a maximum value at ~16 mg/mL, and that is the optimal T161A concentration.

Based on BMEPs and TiO_2 electrophoretic particles, we prepared an electrophoretic suspension and display cell composed of parallel PCB and ITO-covered glass slice filled with the electrophoresis suspension (Figure 7c). The logo of Technical Institute of Physics and Chemistry (TIPC) is on the printed circuit board (PCB). The distance between the two boards is ~100 μm. The electrophoretic suspension containing BMEPs and the TiO_2 particles is filled between the two
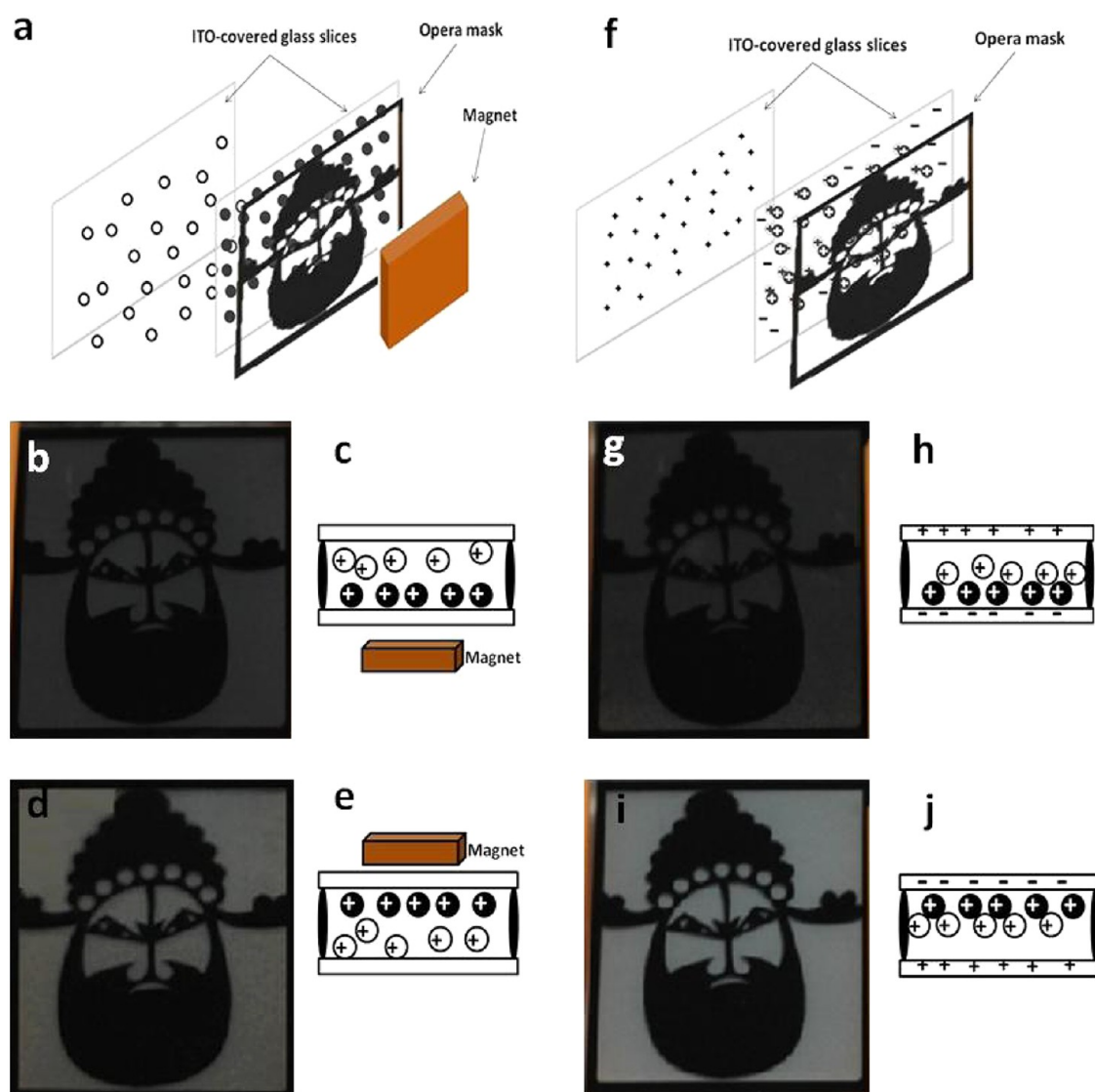
Figure 9. Illustration of the dual-driven electrophoretic display demo device in (a) magnetic drive mode and (f) electronic drive mode. Photographs of the dual-driven display cell with a Traditional Peking Opera Mask film cover: (b) display switch driven by magnetic field above the display, and (c) the corresponding scheme of the electrophoretic display cells; (d) display switch driven by magnetic field below the display, and (e) the corresponding scheme of the electrophoretic display cells; (g) display switch driven by an electronic field above the display, and (h) the corresponding scheme of the electrophoretic display cells; and (i) display switch driven by an electronic field below the display, and (j) the corresponding scheme of the electrophoretic display cells.

baseboards, and the formed device is packaged by UV-curable adhesive. The BMEPs have a mean zeta potential of 15.3 mV. The mean zeta potential of the TiO_2 particles is 5.1 mV. Both the BMEPs and TiO_2 particles are positively charged, but the BMEPs have the higher charge and higher electrophoretic mobility. If the front electrode now has negative charge, both the BMEPs and TiO_2 particles will be attracted to the negative front electrode; because of the higher charge and higher electrophoretic mobility, the BMEPs will reach the front electrode first. Therefore, a layer of BMEPs will coat the front electrode and the medium will appear black to the observer. Conversely, a layer of BMEPs will coat the rear electrode, leaving a layer of TiO_2 particles remote from the rear electrode and facing the observer, so that the medium will appear white to the observer. Figure 7 shows the display result and the drive electronic voltage is 10 V. Since the rear PCB board has a TIPC electrode design, the logo "TIPC" will appear to be black or

while, when the display process is conducted by switching the bias voltage.

This prototype PCB e-paper display shows a high contrast and good visuality without a black and white contrast loss within ~12 h. The black state reflectance is 9.7% and the white state reflectance is ~49%, based on a reflectance measurement by a UV/vis/NIR spectrophotometer under reflection mode with shifting eight times (Figure 8a). The contrast is 5.0. The response time is measured by an Admesy Colorimeter Application, which can record the contrast value of the reflective displays in real time. The result is illustrated in Figure 8b. The time needed to switch the display is <2 s.

The dual-driven display cell is composed of two parallel ITO-covered glass slices, one of which is covered by a Traditional Peking Opera Mask film (Figure 9a). The cell is filled with the as-prepared electrophoretic suspension. By switching on the bias voltage of 10 V, the impression of the Traditional Peking Opera Mask is shown in Figures 9a and 9b. The change of the

electric filed can induce the black and white switch. On the other hand, by moving a magnet over or under the device, the response of the BMEPs to the magnetic field will appear as shown in Figures 9c and 9d. When a magnet is placed upon the device, the BMEPs migrate toward the viewer and the device appears dark. When a magnet is placed under the device, the BMEPs migrate away from the viewer and the white particles become visible to the user. Thus, the Traditional Peking Opera Mask is displayed clearly. The magnet that we have used here is a permanent magnet with a saturation magnetic field of $M_s = 10$ mT. The electric and magnetic fields are applied separately to achieve two approaches of the black and white switch. By driving either the magnetic or electric bias, the display switch is achieved. The contrast under the magnet drive is ~4.0, and the response time in the case of the magnetic switching is ~1 s.

By applying either a magnetic or electronic bias, the black and white switch has a gradually change progress that can be observed by the naked eye. So we can use these electrophoretic display cells into the anticounterfeiting field. The potential advantages for this dual-driven e-paper display application in anticounterfeiting label are (i) it is an optically variable device; (ii) verification of our counterfeit label is completed easily within seconds; (iii) verification is achieved by a battery and magnet without having to use a complicated tool; and (iv) the characteristic of having the feature driven both electrically and magnetically endows the as-prepared demo device with a complicated structure and a double verification method, which can enhance the anticounterfeiting capability.

Therefore, a magnetic-electric dual-driven electronic paper display cell is assembled using BMEPs prepared via an ultrasonic spray pyrolysis process. The BMEPs have appropriate magnet properties and surface functional groups, as well as appropriately low densities to be used as e-paper black pigments. This device could have many promising applications in the security field.

4. CONCLUSION

Herein, we have described the first example of a magnetic-electric dual-driven electronic paper (e-paper), whose switch is achieved by the application of either a bias voltage of 10 V or a magnetic bias via a magnet. The BMEPs suitable for use in the dual-driven e-paper are prepared via an ultrasonic spray pyrolysis process, which is a facile, green, low-cost, one-step method. Fe_3O_4 is the key ingredient of the BMEPs, which endows the black electrophoretic particles with magnetic properties. The solvents and superdispersants are extracted to make a stable electrophoretic suspension. The display developed using this approach possesses characteristics that make it a promising candidate for novel e-papers, which are potentially useful for anticounterfeiting labels.

■ AUTHOR INFORMATION

Corresponding Author
*Tel.: +86-10-82543521. E-mail: mengxw@mail.ipc.ac.cn (X.M.), tangfq@mail.ipc.ac.cn (F.T.).

Author Contributions
The manuscript was written through contributions of all authors. All authors have given approval to the final version of the manuscript.

Notes
The authors declare no competing financial interest.

■ REFERENCES

(1) Ota, I.; Ohishi, J.; Yoshiyama, M. *Proc. IEEE* **1973**, *61*, 832−836.
(2) Comiskey, B.; Albert, J. D.; Yoshizawa, H. *Nature* **1998**, *394*, 253−255.
(3) Shin, S. W.; Yang, H. E. Electrophoretic display and driving method thereof. U.S. Patent 0143700, 2008.
(4) Valianatos, P. J.; Manning, J. J.; Whitesides, T. H.; Walls, M. D. Preparation of capsules. U.S. Patent 0044894, 2010.
(5) Arsenault, A. C.; Puzzo, D. P.; Manners, I.; Ozin, G. A. *Nat. Photon.* **2001**, *1*, 468−472.
(6) Chen, Y.; Au, J.; Kazlas, P.; Ritenour, A.; Gates, H.; McCreary, M. *Nature* **2003**, *423*, 136−136.
(7) Kim, K. S.; Lee, J. Y.; Park, B. J.; Sung, J. H.; Chin, I.; Choi, H. J.; Lee, J. H. *Colloid Polym. Sci.* **2006**, *284*, 813−816.
(8) Werts, M. P. L.; Badila, M.; Brochon, C.; Hebraud, A.; Hadziioannou, G. *Chem. Mater.* **2008**, *20*, 1292−1298.
(9) Meng, X. W.; Tang, F. Q.; Peng, B.; Ren, J. *Nanoscale. Res. Lett.* **2010**, *5*, 174−179.
(10) Li, Z. Y.; Meng, X. W.; Tang, F. Q. *J. Nanosci. Nanotechnol.* **2011**, *11*, 10158−10163.
(11) Heikenfeld, J.; Drzaic, P.; Yeo, J. S.; Koch, T. *J. SiD* **2011**, *19*, 129−156.
(12) Badila, M.; Hebraud, A.; Brochon, C.; Hadziioannou, G. *ACS. Appl. Mater. Interfaces* **2011**, *3*, 3602−3610.
(13) Peng, B.; Meng, X. W.; Tang, F. Q.; Ren, X. L.; Chen, D. *J. Phys. Chem. C* **2009**, *113*, 20240−20245.
(14) Yu, D. G.; An, J. H.; Bae, J. Y.; Ahn, S. D.; Kang, S. Y.; Suh, K. S. *Macromolecules* **2005**, *38*, 7485−7491.
(15) Cho, S. H.; Kwon, Y. R.; Kim, S. K.; Noh, C. H.; Lee, J. Y. *Polym. Bull.* **2007**, *59*, 331−338.
(16) Kim, M. K.; Kim, C. A.; Ahn, S. D.; Kang, S. R.; Suh, K. S. *Synth. Met.* **2004**, *146*, 197−199.
(17) Yu, D. G.; An, J. H. *Colloid. Surf. A* **2004**, *237*, 87−93.
(18) Duan, J. H.; Feng, Y. Q.; Yang, G.; Xu, W. L.; Li, X. G.; Liu, Y.; Zhao, J. *Ind. Eng. Chem. Res.* **2009**, *48*, 1468−1475.
(19) Peng, B.; Meng, X. W.; Tang, F. Q.; Ren, J.; Chen, D.; Ren, X. L. *J. Colloid Interface Sci.* **2009**, *329*, 62−66.
(20) Meng, X. W.; Wen, T.; Sun, S. W.; Zheng, R. B.; Ren, J.; Tang, F. Q. *Nanoscale. Res. Lett.* **2010**, *5*, 1664−1668.
(21) Wen, T.; Meng, X. W.; Li, Z. Y.; Ren, J.; Tang, F. Q. *J. Mater. Chem.* **2010**, *20*, 8112−8117.
(22) Zheng, R. B.; Meng, X. W.; Tang, F. Q. *Eur. J. Inorg. Chem.* **2009**, *20*, 3003−3007.
(23) Cao, F.; Chen, C.; Wang, Q.; Chen., Q. *Carbon* **2007**, *45*, 727−731.
(24) Nasrazadani, S.; Raman., A. *Corros. Sci.* **1993**, *34*, 1355−1365.
(25) Haerle, R.; Riedo, E.; Pasquarello, A.; Baldereschi, A. *Phys. Rev. B* **2001**, *65*, 045101-1−045101-9.
(26) Lee, B. I.; Paik, U. *Ceram. Int.* **1993**, *19*, 241−250.
(27) Hsiang, H. I.; Chen, C. C.; Tsai, J. Y. *Appl. Surf. Sci.* **2005**, *245*, 252−259.
(28) Nasu, A.; Otsubo, Y. *J. Colloid. Interf. Sci.* **2006**, *296*, 558−564.
(29) Ghosh, S.; Jiang, W.; McClements, J. D.; Xing, B. *Langmuir* **2011**, *27*, 8036−8043.
(30) Farrokhpay, S. *Adv. Colloid Interface Sci.* **2009**, *151*, 24−32.